σ-Borane Complexes of Manganese and Rhenium

Sabine Schlecht and John F. Hartwig*

Contribution from the Department of Chemistry, Yale University, P.O. Box 208107, New Haven, Connecticut 06520-8107

Received May 4, 2000

Abstract: The late transition metal borane complexes (MeCp)Mn(CO)$_2$(HBR$_2$) (R = alkyl, alkoxy) and Cp*Re(CO)$_2$(HBpin) (HBpin = pinacolborane, Cp* = pentamethylcyclopentadienyl) have been synthesized and isolated. All complexes were characterized spectroscopically, and X-ray crystal structure analyses were performed for (MeCp)Mn(CO)$_2$(HBpin), (MeCp)Mn(CO)$_2$(HBcat) (HBcat = catecholborane) and (MeCp)Mn(CO)$_2$(HBCy$_2$) (Cy = cyclohexyl). These data show that the complexes contain a borane ligand with a weakened but intact B−H bond. The borane ligand in (MeCp)Mn(CO)$_2$(HBcat) is replaced by PhCCPh, Ph$_3$SnH, Ph$_2$MeSiH, CO, and excess HBpin in ligand substitution reactions. The mechanism of substitution by PhCCPh was investigated. Kinetic studies showed that the reaction is first-order in complex and that borane and PhCCPh react competitively with the 16-electron intermediate, (MeCp)Mn(CO)$_2$. The $\Delta H^{\ddagger}$ value for borane dissociation was 24 ± 3 kcal/mol for (MeCp)Mn(CO)$_2$(HBcat) and 21 ± 1 kcal/mol for (MeCp)Mn(CO)$_2$(HBCy$_2$), which provided an upper limit on the metal−borane binding energies. Dynamic NMR spectroscopy of (MeCp)Mn(CO)$_2$(HBcat) revealed two types of rotations of the borane ligand.

Introduction

σ-Complexes[1−4] are reactive intermediates that typically precede oxidative addition of substrates with an X−H bond.[1] σ-Complexes are, therefore, intermediates in catalytic hydrogenation,[5] hydrosilylation,[6,7] and hydroboration[8] reactions. In contrast to the large number of dihydrogen complexes[9] and σ-silane compounds,[6,7] monoborane σ-complexes are limited in number and have been isolated only recently.[10−13] They are the only simple, isolable H−X σ-complex containing a single first-row element X. Alkane complexes have been detected spectroscopically in solution,[14] in the gas phase,[15] and by matrix isolation,[16,17] but the only isolated alkane complex contains a hydrocarbon that is held in place, perhaps principally, by hydrophobic interactions with a double-A-frame porphyrin ligand.[18]

The isolation and characterization of σ-complexes contributes to our understanding of the bonding interactions between substrates with X−H bonds and unsaturated transition-metal compounds. Silane, dihydrogen, and now borane complexes are stabilized by exceptionally strong interactions between the metal center and the H−X bond. Thus, a precise electronic description of stable σ-compounds can help us to understand what controls the strength of these complexes when they act as reaction intermediates and cannot be isolated.

Puddephatl[19a] and, more recently, Shimoi[19b] reported phosphine-ligated boryl complexes (R$_3$PH$_2$B−M). The hydrogen atoms of these complexes, however, point away from the metal center. These complexes are, therefore, more akin to Lewis acid−base adducts of boryl complexes than to the σ-borane complexes reported here. Shimoi has also reported complexes of phosphinoboranes R$_3$PBH$_3$.[13] In this case no metal−boron interaction was detected, again distinguishing them from the σ-complexes of three-coordinate boranes which are reported here.

We felt that borane complexes of manganese, such as (MeCp)Mn(CO)$_2$(HBR$_2$), were important synthetic targets because they would allow one to make comparisons to early transition-metal borane complexes which have been prepared recently and to silane, (MeCp)Mn(CO)$_2$(HSiR$_3$), and stannane, (MeCp)Mn(CO)$_2$(HSnR$_3$), complexes, which are the original σ-complexes.[3,20] To allow for such comparisons, our investigations addressed the influence of the borane substituents on the three-center bonding interaction, the strength of the metal−borane interactions, and the mechanism of the displacement of borane by more strongly coordinating dative ligands.

* To whom correspondence should be addressed.

(1) Crabtree, R. H. *Angew. Chem., Int. Ed. Engl.* **1993**, *32*, 789.
(2) Schubert, U. *Adv. Organomet. Chem.* **1990**, *30*, 151.
(3) Schubert, U.; Scholz, G.; Müller, J.; Ackermann, K.; Wörle, B. *J. Organomet. Chem.* **1986**, *306*, 303.
(4) Buchanan, J. M.; Stryker, J. M.; Bergman, R. G. *J. Am. Chem. Soc.* **1986**, *108*, 1537.
(5) Halpern, J. *Science* **1982**, *217*, 401.
(6) Chalk, A. J.; Harrod, J. F. *J. Am. Chem. Soc.* **1965**, *87*, 16.
(7) Sommer, L. H.; Lyons, J. E.; Fujimoto, H. *J. Am. Chem. Soc.* **1969**, *91*, 2670.
(8) Beletskaya, I.; Pelter, A. *Tetrahedron* **1997**, *53*, 4957.
(9) Kubas, G. J. *Acc. Chem. Res.* **1988**, *21*, 120.
(10) Hartwig, J. F.; Muhoro, C. N.; He, X. *J. Am. Chem. Soc.* **1996**, *118*, 10936.
(11) Muhoro, C. N.; Hartwig, J. F. *Angew. Chem., Int. Ed. Engl.* **1997**, *36*, 1510.
(12) Muhoro, C. N.; He, X.; Hartwig, J. F. *J. Am. Chem. Soc.* **1999**, *121*, 5033.
(13) Shimoi, M.; Nagai, S.; Ichikawa, M.; Kawano, Y.; Katoh, K.; Uruichi, M.; Ogino, H. *J. Am. Chem. Soc.* **1999**, *121*, 11704.
(14) Geftakis, S.; Ball, G. E. *J. Am. Chem. Soc.* **1998**, *120*, 9953.
(15) Brown, C. E.; Ishikawa, Y.-I.; Hackett, P. A.; Rayner, D. M. *J. Am. Chem. Soc.* **1990**, *112*, 2530.
(16) Rest, A. J.; Whitwell, I.; Graham, W. A. G.; Hoyano, J. K.; McMaster, A. D. *J. Chem. Soc.* **1987**, 1181.
(17) Turner, J. J.; Burdett, J. K.; Perutz, R. N.; Poliakoff, M. *Pure Appl. Chem.* **1977**, *49*, 271.
(18) Evans, D. R.; Drovetskaya, T.; Reed, C. A.; Boyd, P. D. W. *J. Am. Chem. Soc.* **1997**, *119*, 3633.
(19) (a) Elliot, D. J.; Levy, C. J.; Puddephatl, R. J.; Holah, D. G.; Hughes, A. N.; Magnesun, V. R.; Moser, I. M. *Inorg. Chem.* **1990**, *29*, 5015. (b) Kawano, Y.; Yasue, T.; Shimoi, M. *J. Am. Chem. Soc.* **1999**, *121*, 11744.
(20) Graham, W. A. G.; Jetz, W. *Inorg. Chem.* **1971**, *10*, 4.

10.1021/ja001546o CCC: $19.00
Published on Web 09/13/2000

Scheme 1

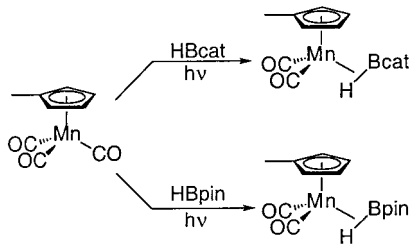

Scheme 2

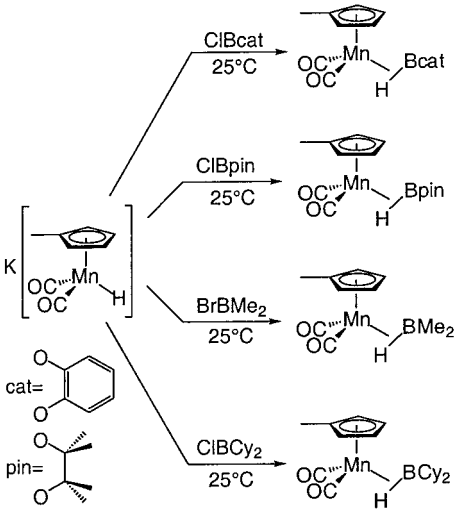

Results

Synthesis and Structures of (MeCp)Mn(CO)$_2$(HBcat) (1) and (MeCp)Mn(CO)$_2$(HBpin) (2). Borane complexes of the (MeCp)Mn(CO)$_2$ fragment were generated by photolysis of (MeCp)Mn(CO)$_3$ and by nucleophilic substitution using [(MeCp)Mn(CO)$_2$H]$^-$, as shown in Schemes 1 and 2. Photolysis of (MeCp)Mn(CO)$_3$ in THF for 30 min in the presence of a large excess (14−16 equiv) of the corresponding borane produced (MeCp)Mn(CO)$_2$(HBcat) (**1**) in 53% yield and (MeCp)-Mn(CO)$_2$(HBpin) (**2**) in 18% yield as yellow solids after recrystallization from pentane. The use of THF as a solvent was essential, presumably because of its ability to stabilize the photolytically generated (MeCp)Mn(CO)$_2$. The reaction of either ClBcat or ClBpin generated in situ with the known anionic manganese hydride K[(MeCp)Mn(CO)$_2$H][21] in pentane at room temperature (Scheme 2) provided an alternative route that formed **1** and **2** in higher yields. The reaction was complete after 10 min and gave 92% yield of (MeCp)Mn(CO)$_2$(HBcat) and 65% yield of (MeCp)Mn(CO)$_2$(HBpin).

(MeCp)Mn(CO)$_2$(HBcat) was stable at room temperature as a solid, but decomposed slowly in solution. The pinacolborane derivative decomposed at room temperature over hours, even as a solid, but was stored at −30 °C for an extended period of time without decomposition.

The ^{11}B NMR shifts of both **1** and **2**, 46 ppm for **1** and 45 ppm for **2**, were far downfield from those of the the free boranes. High-field signals at −14.46 ppm for **1** and −15.66 ppm for **2** were observed in the ^{1}H NMR spectrum. These hydride resonances were broad, due to the proximity of the boron atom, and sharpened upon ^{11}B decoupling (Figure 1). The scalar coupling constants, $^1J(^1\mathrm{H},^{11}\mathrm{B})$, were approximately 95 Hz in both complexes, which is roughly half the value found in the free boranes. The deuterated compound (MeCp)Mn(CO)$_2$-(DBcat) (**1-d**) showed a ^{2}H NMR chemical shift that was indistinguishable from that of the hydride resonance in protiated **1**; no isotopic perturbation on the chemical shift was observed.[22] The IR spectrum of **1** contained a broad band at 1606 cm^{-1}, most likely corresponding to the H−Mn stretching frequency, with the B−H stretch at low frequency, as seen for silane complexes.[23] Strong bands at 1995 cm^{-1} (ν_sCO) and 1937 cm^{-1} (ν_{as}CO) were observed for the carbonyl stretches. Similar bands at 1603 cm^{-1} (νHB), 1983 cm^{-1} (ν_sCO), and 1921 cm^{-1} (ν_{as}-CO) were observed for pinacolborane complex **2**.

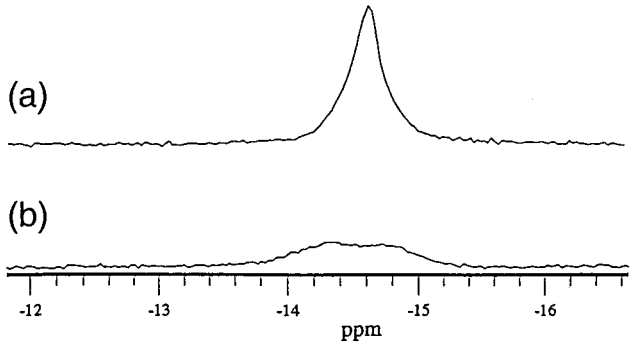

Figure 1. ^{1}H NMR resonance of the hydride in **1** at 25 °C (a) with and (b) without ^{11}B decoupling.

Complexes **1** and **2** were also characterized by X-ray crystallography. The two complexes showed similar connectivity and structural properties. Acquisition parameters are given in Table 1, selected bond distances and angles are given in Tables 2 and 3, and ORTEP diagrams of **1** and **2** are provided in Figures 2 and 3. The metal-bound hydrogen atom was found in the difference Fourier map of both complexes and was refined. Both complexes contain extremely small H−Mn−B angles of 37.2-(8)° and 38.2(6)°. The Mn−B distances of 2.083(2) Å in **1** and 2.149(2) Å in **2** were longer than those in the related boryl complexes CpFe(CO)$_2$(Bcat) [d(Fe−B) = 1.96 Å] or CpFe-(CO)$_2$(BPh$_2$) [d(Fe−B) = 2.03 Å].[24] The B−H bond lengths of 1.29(2) Å in the HBcat complex **1** and 1.31(2) Å in the HBpin complex **2** are between the value of 1.26 Å found in Cp$_2$Ti-(HBcat)$_2$ and that of 1.35 Å in Cp$_2$Ti(HBcat-3-F)(PMe$_3$), the only other crystallographically characterized σ-borane complexes of three-coordinate boron.[12] These values for **1** and **2** are significantly longer than the 1.17 Å distances calculated for catecholborane and the closely related cyclic alkoxyboranes.[25]

Synthesis and Structure of (MeCp)Mn(CO)$_2$(HBR$_2$) (R = Me, Cy) (3, 4). Reaction of photochemically generated (MeCp)-Mn(CO)$_2$ with dialkylboranes did not occur, presumably due to the dimeric structures of these boranes. However, the desired dialkylborane complexes were formed by the reaction of the manganese anion with halodialkylboranes as shown in Scheme 2. (MeCp)Mn(CO)$_2$(HBMe$_2$) (**3**) was obtained in 82% yield by reacting K[(MeCp)Mn(CO)$_2$H] with BrBMe$_2$ in pentane at room temperature. The dicyclohexylborane complex **4** was prepared in a similar manner from the hydridomanganate and ClBCy$_2$ in 85% yield. Complex **3** was a red oil that was judged pure by ^{1}H, ^{13}C, and ^{11}B NMR spectroscopy. Cyclohexylborane complex **4** was as a red solid. Compound **3** decomposed quickly at room temperature. Compound **4** was stable at room temperature for

(21) Braunschweig, H.; Ganter, B. *J. Organomet. Chem.* **1997**, *545*, 163.

(22) Hartwig, J. F.; DeGala, S. R. *J. Am. Chem. Soc.* **1994**, *116*, 3661.

(23) Delpech, F.; Sabo-Etienne, S.; Daran, J. C.; Chandret, B.; Hussein, K.; Marsden, C. J.; Barthelat, T. C. *J. Am. Chem. Soc.* **1999**, *121*, 6668.

(24) Hartwig, J. F.; Huber, S. *J. Am. Chem. Soc.* **1993**, *115*, 4908.

(25) The distances were calculated from **z**-matrices in Roblen, P. R.; Hartwig, J. F. *J. Am. Chem. Soc.* **1996**, *118*, 4648.

Table 1. Acquisition Parameters for **1**, **2**, and **4**

empirical formula	$C_{14}H_{12}BO_4Mn$ (**1**)	$C_{14}H_{20}BO_4Mn$ (**2**)	$C_{20}H_{30}BO_2Mn$ (**4**)
formula weight	309.99	318.06	368.20
color of crystal	yellow	yellow	red
crystal system	triclinic	monoclinic	triclinic
space group	$P\bar{1}$	$P2_1/a$	$P\bar{1}$
unit cell dimension	$a = 7.7712(4)$ Å	$a = 12.6474(3)$ Å	$a = 6.7421(3)$ Å
	$b = 9.5508(4)$ Å	$b = 10.0519(3)$ Å	$b = 9.3350(3)$ Å
	$c = 9.7226(4)$ Å	$c = 12.8851(4)$ Å	$c = 16.1767(5)$ Å
	$\alpha = 101.005(3)°$		$\alpha = 95.464(3)°$
	$\beta = 108.881(2)°$	$\beta = 115.635(2)°$	$\beta = 90.115(2)°$
	$\gamma = 97.727(2)°$		$\gamma = 107.928(2)°$
Z value	2	4	2
goodness-of-fit	1.64	2.92	2.27
final R indices	$R = 0.030$	$R = 0.031$	$R = 0.037$
	$R_w = 0.044$	$R_w = 0.049$	$R_w = 0.050$

Table 2. Selected Bond Distances in **1**, **2**, and **4**

	distance (Å)		
bond	**1**	**2**	**4**
Mn−B	2.083(2)	2.149(2)	2.187(3)
Mn−H(1)	1.57(2)	1.53(2)	1.49(2)
B−H(1)	1.29(2)	1.31(2)	1.24(2)
B−O(3) or B−C(9)	1.413(2)	1.376(2)	1.590(3)
B−O(4) or B−C(15)	1.404(2)	1.376(2)	1.590(3)

Table 3. Selected Bond Angles in **1**, **2**, and **4**

			angle (deg)		
atom	atom	atom	**1**	**2**	**4**
H(1)	Mn	B	38.2(6)	37.2(8)	33.2(7)
Mn	B	H(1)	48.6(7)	44.7(9)	41.1(9)
C(1)	Mn	C(2)	90.66(7)	90.32(7)	93.4(1)
O(3) or C(9)	B	O(4) or C(15)	109.8(1)	112.7(1)	117.9(2)

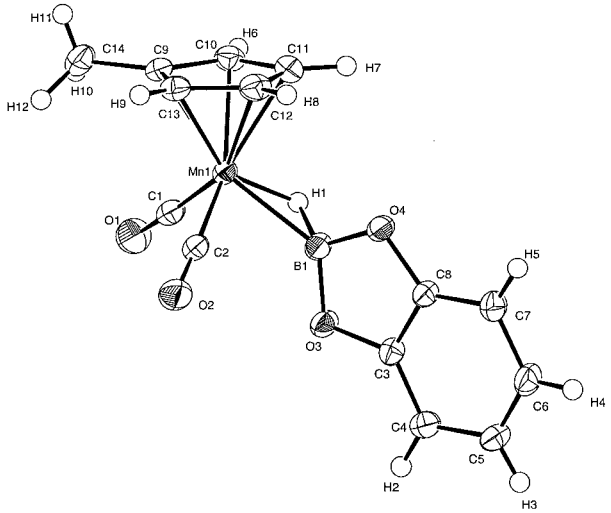

Figure 2. ORTEP diagram of **1**.

several hours, but decomposed within 1 day when in solution and as a solid.

The ^{11}B NMR resonances for **3** and **4** were broad singlets at 101 and 104 ppm. Like **1** and **2**, the dialkylborane complexes showed high-field signals in the ^{1}H NMR spectrum for the hydride. A broad singlet at −17.06 ppm was observed for dimethyl **3**, and a broad singlet at −16.96 ppm was detected for dicyclohexyl **4**. In both cases, the hydride signal sharpened upon ^{11}B-decoupling, indicating the presence of a scalar coupling between the boron and the hydrogen atoms. The IR spectrum of **3** in hexanes showed an IR band at 1592 cm^{-1} and carbonyl

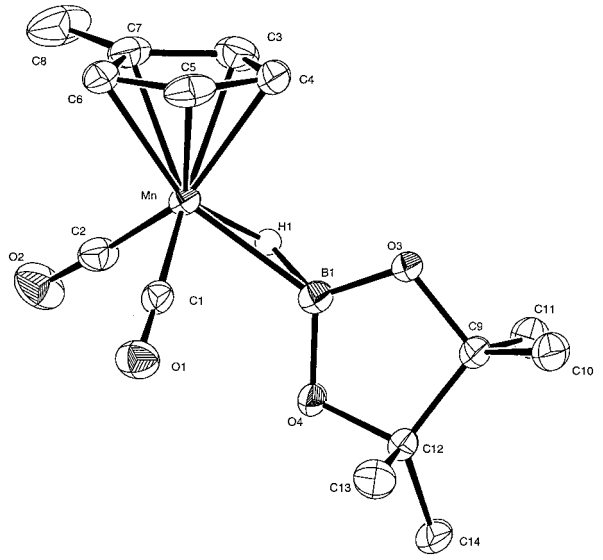

Figure 3. ORTEP diagram of **2**.

bands at 1975 and 1910 cm^{-1}. Similar values for **4** at 1597 cm^{-1}, 1967 cm^{-1} (ν_sCO), and 1901 cm^{-1} (ν_{as}CO) were observed.

Complex **4** was also characterized by X-ray crystallography. Acquisition parameters are given in Table 1, selected bond distances and angles are given in Tables 2 and 3, and an ORTEP diagram of **4** is provided in Figure 4. As for **1** and **2**, the metal-bound hydrogen atom was located in the difference Fourier map and was refined. The Mn−B distance of 2.19 Å is longer than that in the alkoxyborane complexes **1** and **2**, and the Mn−H bond is shortened to 1.49 Å. The B−H distance of 1.24 Å in **4** appeared shorter than that in the two alkoxyborane complexes, but the difference in bond lengths is close to two standard deviations (Table 2). If significant, the shorter bond distance would be caused by differences in metal−ligand interaction, because a free monomeric dialkylborane is computed to have a slightly longer, 1.20 Å, B−H distance than the 1.17 Å distance in a free dialkoxyborane.[25] The overall structural features clearly indicate a weaker metal−boron interaction and a more pronounced hydride character for the borane hydrogen.

Synthesis of Cp*Re(CO)$_2$(HBpin) (5). A synthetic pathway different from those for the manganese complexes was used to prepare Cp*Re(CO)$_2$(HBpin) (**5**). The reaction of *cis*-Cp*Re(CO)$_2$(Bpin)$_2$[26] with methanol or neopentyl alcohol in benzene at room temperature gave **5** in quantitative yield after 2 h. The compound is a colorless solid that was stable at room temper-

(26) Chen, H.; Hartwig, J. F. *Angew. Chem., Int. Ed. Engl.* **1999**, *38*, 3391.

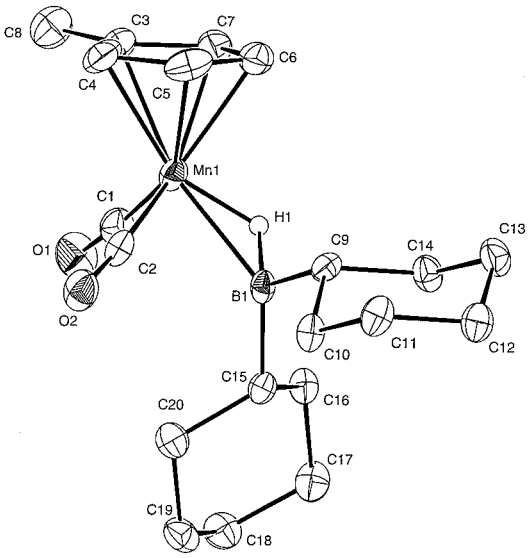

Figure 4. ORTEP diagram of **4**.

Scheme 3

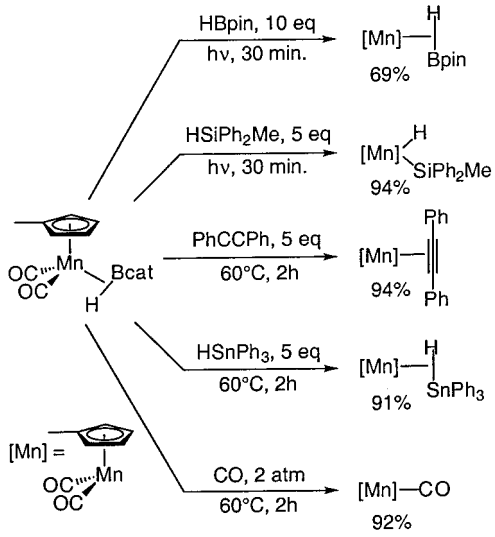

ature. A broad singlet was observed for the hydrogen of the coordinated borane in the ^{1}H NMR spectrum at −11.06 ppm. Compound **5** resonated at 46 ppm in the ^{11}B NMR spectrum. The IR bands were similar to those of the manganese compounds and were found at 1603 cm^{-1}, 1981 cm^{-1} (ν_sCO), and 1924 cm^{-1} (ν_{as}CO). Crystals suitable for X-ray diffraction were not obtained, despite repeated attempts.

Ligand-Substitution Reactions of (MeCp)Mn(CO)$_2$(HBcat) (1). The catecholborane in **1** was replaced by a variety of ligands under both photochemical and thermal conditions. Scheme 3 summarizes the ligand-substitution reactions. All of these reactions were conducted in the presence of at least 5 equiv of incoming ligand to minimize dimerization of the potential intermediate, (MeCp)Mn(CO)$_2$, which forms the insoluble [(MeCp)Mn(CO)$_2$]$_2$. Except for the conversion of **1** to **2**, which was conducted in THF, all reactions were carried out in benzene solvent.

Thermal dissociation of catecholborane required a temperature of 60 °C. Diphenylacetylene displaced the catecholborane ligand and formed the previously described[27] [(MeCp)Mn(CO)$_2$(η^2-PhCCPh)] in 94% yield. Reaction with 2 atm of CO at 60 °C for 2 h gave (MeCp)Mn(CO)$_3$ in 92% yield. Reactions with HBpin and Ph$_2$MeSiH were conducted photochemically because the products are not stable at 60 °C. Irradiation of **1** for 30 min using a mercury-arc lamp in the presence of 10 equiv of HBpin gave complex **2** in 69% yield. Reaction of **1** with Ph$_2$MeSiH under similar conditions gave (MeCp)Mn(CO)$_2$(SiPh$_2$Me)(H)[21] in 94% yield. For all ligand-substitution reactions that we conducted, the conversion of (MeCp)Mn(CO)$_2$(HBcat) was higher than 95%. The amount of side products never exceeded 10%.

(27) Strohmeier, W.; Laporte, H.; v. Hobe, D. *Chem. Ber.* **1962**, *95*, 455.

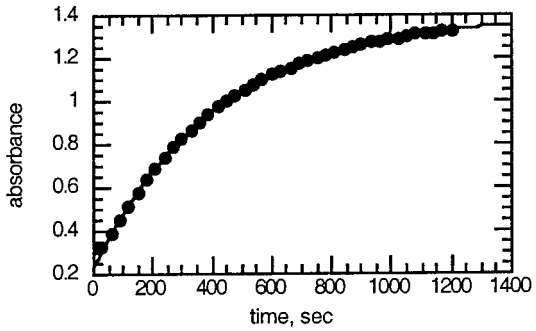

Figure 5. Formation of diphenylacetylene complex, monitored at λ = 420 nm.

Table 4. Observed Rate Constants at Different Concentrations of Catecholborane and Diphenylacetylene; T = 70 °C

[**1**], mmol/L	[HBcat], mmol/L	[PhCCPh], mmol/L	k_{obs} ($\cdot 10^4$, s^{-1})
0.645	3.188	9.719	14.0
0.645	12.750	9.719	12.0
0.645	25.500	9.719	10.1
0.645	51.000	9.719	7.9
0.645	76.500	9.719	6.7
0.242	4.688	1.873	11.3
0.242	4.688	3.745	13.1
0.242	4.688	7.491	16.3
0.242	4.688	14.981	17.2
0.242	4.688	59.925	18.9
0.242	4.688	119.850	18.9

Kinetic Studies of the Reactions of (MeCp)Mn(CO)$_2$-(HBcat) (1) and (MeCp)Mn(CO)$_2$(HBCy$_2$) (4) with PhCCPh. Kinetic studies of the reaction of **1** with diphenylacetylene were conducted to determine the mechanism of this process and to obtain an upper limit on the Mn−(HBcat) dative bond energy. The kinetic measurements were made using UV/vis spectroscopy, monitoring the band at 420 nm, due to the absorption of the orange diphenylacetylene complex, which was formed in the reaction. The reactions were run in toluene at 70 °C. As indicated by the excellent fit to a single exponential for the formation of the product (Figure 5), the substitution of catecholborane by diphenylacetylene was first-order in the borane complex. As shown by the rate constants in Table 4, the observed rate constant depended on the concentration of both the added borane and the incoming ligand. The reaction rate increased with increasing concentrations of diphenylacetylene when the ratio of alkyne to HBcat was low. However, saturation of the reaction rate was observed at high concentrations of [PhCCPh] (Figure 6). Added catecholborane inhibited the ligand exchange at low alkyne/borane ratios. A plot of $1/k_{obs}$ versus the concentration of catecholborane at constant alkyne concentration is provided in Figure 7.

The temperature dependence of the reaction rate for displacement of HBcat and HBCy$_2$ was evaluated, and activation parameters were determined to obtain an upper limit on the binding energies of HBcat and HBCy$_2$ to the metal fragment.

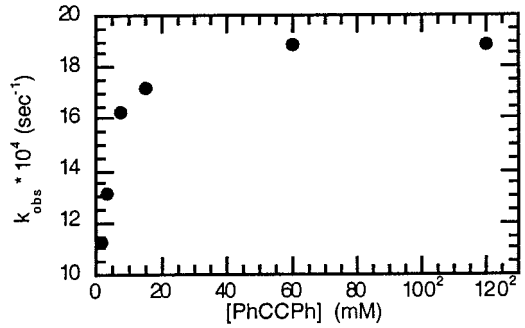

Figure 6. k_{obs} versus the concentration of diphenylacetylene.

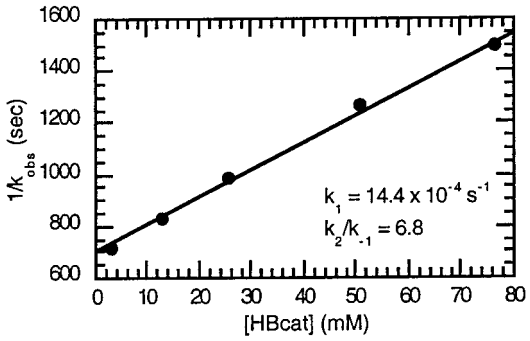

Figure 7. $1/k_{obs}$ versus the concentration of catecholborane.

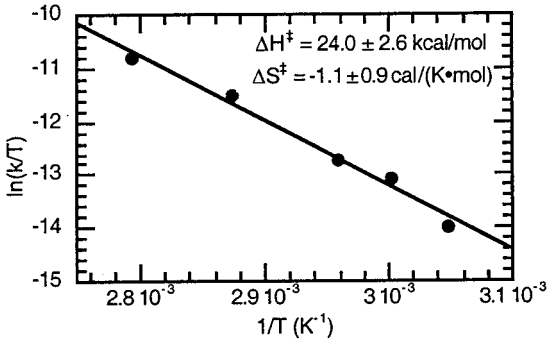

Figure 8. Eyring plot for the reaction of $(MeCp)Mn(CO)_2(HBcat)$ with PhCCPh.

For the reaction of the catecholborane complex, rate constants were measured from 55 to 85 °C for the following concentrations of reactants: [**1**] = 0.45 mM, [HBcat] = 8.35 mM, and [PhCCPh] = 29.50 mM. These concentrations were chosen such that $k_{obs} = k_1$, the rate for borane dissociation (see discussion). The Eyring plot (Figure 8), provided the activation parameters $\Delta H^‡ = 24.0 \pm 2.6$ kcal/mol and $\Delta S^‡ = -1.1 \pm 0.9$ eu. For the reaction of the dicyclohexylborane complex **4** with diphenylacetylene, rate constants were measured from 25 to 55 °C, with [**4**] = 0.68 mM, [PhCCPh] = 50.95 mM, and no added dicyclohexylborane, because the free borane is a dimer. As in the case of the catecholborane complex, these conditions ensure that $k_{obs} = k_1$. The reaction was first-order in borane complex. The Eyring plot (Figure 9) provided the activation parameters $\Delta H^‡ = 21.0 \pm 1.1$ kcal/mol and $\Delta S^‡ = -5.9 \pm 3.3$ eu. The displaced dicyclohexylborane reacted immediately with the excess diphenylacetylene to form the hydroboration product dicyclohexyl-*cis*-1,2-diphenyl(vinyl)borane. The identity of this side product was confirmed by comparing the ^{1}H and ^{11}B NMR spectra to those of material formed from the addition of diphenylacetylene and dimeric dicyclohexylborane in a separate reaction.

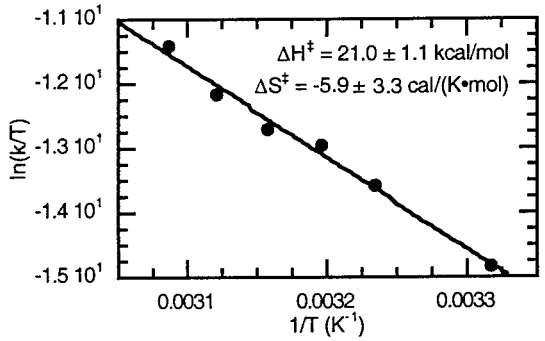

Figure 9. Eyring plot for the reaction of $(MeCp)Mn(CO)_2(HBCy_2)$ with PhCCPh.

Discussion

Spectroscopic and Structural Studies. X-ray diffraction, in combination with NMR and IR spectroscopy, was used to understand how free neutral boranes bind to the manganese and rhenium fragments. In short, the crystallographic and spectroscopic data show direct bonding between the metal (Mn or Re) and boron, between the metal and hydrogen, and between boron and hydrogen. This section of the discussion is organized according to the different bonding interactions and the spectroscopy that support their existence.

1. Evidence for B−H Bonding. Several lines of data support B−H bonding. First, the crystal structures of **1**, **2,** and **4** supported the presence of this interaction. All three complexes showed a lateral configuration in a four-legged piano-stool geometry with OC−Mn−CO angles which were near 90°. In diagonal dicarbonyl complexes, angles of 100−110° are typically found.[28,29] The H−Mn−B angles were small (33−38°) and are inconsistent with a structure that would be described by a Mn(III) center containing a boryl group and a hydrogen in two separate coordination sites. Consistent with this small angle, B−H bond lengths were between 1.24(2) and 1.31(2) Å. These values are clearly within B−H bonding distance but are elongated relative to the 1.17 and 1.20 Å distances calculated for related free boranes.[25]

A direct bonding interaction between boron and hydrogen was also shown clearly by ^{1}H{^{11}B} and by ^{11}B NMR spectroscopy. Scalar coupling between the boron and the hydride was observed directly by ^{11}B NMR spectroscopy for compounds **1** and **2**, and the coupling constants of 95 Hz were too large for a scalar coupling solely through the metal. Known complexes with two discrete *cis*-boryl and hydride ligands do not show any evidence for scalar coupling; sharp hydride signals are observed for those compounds.[30] In addition, the ^{1}H NMR signals for the hydrides of **1** and **2** were broad and sharpened upon boron decoupling. The half-width and the shape of the borane hydride resonances showed a strong temperature dependence for all complexes. This phenomenon is well-known for BH_4^- complexes[31] and other compounds that contain a proton bound to a quadrupolar nucleus.[32] This "virtual self-decoupling"[31] gave additional, indirect evidence for scalar coupling between the boron and the hydrogen atoms.

(28) Dong, D. F.; Hoyano, J. K.; Graham, W. A. G. *Can. J. Chem.* **1981**, *59*, 1455.
(29) Smith, R. A.; Bennett, M. J. *Acta Crystallogr. Sect. B* **1977**, *33*, 1113.
(30) Irvine, G. J.; Lesley, G.; Marder, T. B.; Norman, N. C.; Rice, C. R.; Robins, E. G.; Roper, W. R.; Whitell, G. R.; Wright, L. J. *Chem. Rev.* **1998**, *98*, 2685.
(31) Marks, T. J.; Shimp, L. A. *J. Am. Chem. Soc.* **1972**, *94*, 1542.
(32) Pople, J. A. *Mol. Phys.* **1958**, *1*, 168.

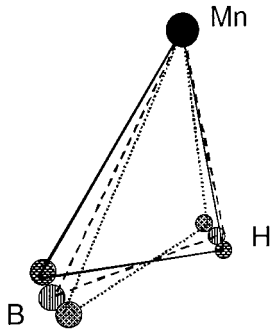

: HBcat : HBpin : $HBCy_2$

Figure 10. Core geometries in borane complexes **1**, **2**, and **4**.

IR spectroscopy provided information about the B−H bond order. IR bands between 1606 cm^{-1} (**1**) and 1592 cm^{-1} (**3**) corresponded to a stretching mode involving the hydride, which is likely to be predominantly M−H in character. The B−H stretches are even lower in frequency and much lower in energy than the B−H-stretching frequency in free monomeric boranes (2660 cm^{-1} for catecholborane). These data indicated a reduced B−H bond order. Rhenium HBpin complex **5** showed the same IR pattern as the manganese analogue **2**, indicating a similar reduction in B−H bond order. Thus, borane complex **5** contains a partial H−X bond, in contrast to the silicon analogue $CpRe(CO)_2(H)(SiPh_3)$,[28,29] which contains H and $SiPh_3$ as two individual ligands.

2. Evidence for M−B Bonding. The X-ray structures of **1**, **2**, and **4** showed evidence for a partial M−B bond order. The bond lengths of 2.083(2) Å in **1** and 2.149(2) Å in **2** are certainly within M−B bonding distance but are longer than those in the related boryl complexes $CpFe(CO)_2(Bcat)$ [d(Fe−B) = 1.96 Å] or $CpFe(CO)_2(BPh_2)$ [d(Fe−B) = 2.03 Å].[24] The presence of a metal−boron bond was also established by the ^{11}B NMR chemical shifts of the complexes (45−46 ppm for dialkoxyboranes and 101−104 ppm for dialkylboranes). The chemical shifts are located far downfield from the ^{11}B NMR signals of monomeric, free boranes or Lewis base adducts of dialkylboranes.[33] The ^{11}B NMR chemical shifts lie near those of the resonances for boryl complexes such as $[Mn(CO)_5(Bcat)]$ (43 ppm), $[CpFe(CO)_2(Bcat)]$ (52 ppm), and $[CpFe(CO)_2(BPh_2)]$ (121 ppm).[24]

3. Evidence for M−H Bonding. Direct M−H bonding was confirmed by the high-field ^1H NMR shifts of the hydrogen atoms of the coordinated boranes. These resonances are at a higher field than those of four-coordinate hydridoborates or Lewis acid−base adducts of boranes.[33] The assignment of the extreme high-field ^1H NMR signals to the borane hydrogen was confirmed by the use of DBcat in the synthesis of **1-*d*$_1$**. A ^2H NMR signal was observed at the same chemical shift as its protiated analogue **1**. The hydride ligands were also identified by X-ray diffraction, and the observation of M−H bond distances between 1.49(2) and 1.57(2) Å indicated a direct M−H bond.

4. Comparison of Overall Structural Features for the Three Complexes. Figure 10 shows changes in core geometry, determined by X-ray diffraction, for the three complexes. In the series of compounds **1**, **2**, and **4**, the center of the B−H bond is roughly equidistant from the metal center, but the M−B distance is lengthened and the M−H distance is shortened in **2** and **4** relative to the distances in **1**. Catecholborane complex **1** showed the most typical η^2, side-on geometry. The borane ligand in pinacolborane complex **2** is pivoted relative to that in **1** to create a Mn−B bond that is elongated by 0.07 Å and an Mn−H distance that is shortened by 0.04 Å relative to that in **1**. The borane in cyclohexyl complex **4** is further pivoted to create an Mn−B distance that is 0.04 Å longer and an Mn−H distance that is 0.04 Å shorter than those in **2**.

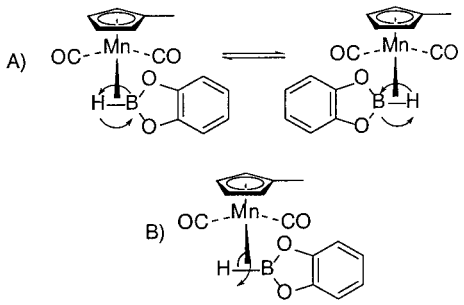

Figure 11. Intramolecular motions in complex **1**.

The IR-stretching frequencies for the CO groups were sensitive to the identity of the borane. The νCO values were higher for the alkoxyborane complexes **1** and **2** than for the dialkylborane complexes **3** and **4**. The values of 1995 cm^{-1} (ν_sCO) and 1937 cm^{-1} (ν_{as}CO) for the catecholborane complex **1** indicated that HBcat is a weaker donor and a stronger acceptor in complex **1** than is HBpin in complex **2**, for which stretching frequencies of 1983 cm^{-1} (ν_sCO) and 1921 cm^{-1} (ν_{as}CO) were found. The carbonyl stretching frequencies of **3** and **4** suggested that dimethylborane and dicyclohexylborane were even stronger σ-donating and weaker π-accepting ligands than pinacolborane. A more electron-rich B−H bond that acts as a stronger donor to the metal may override increases in Lewis acidity that would be expected for the dialkylborane ligands.

Both the core structure and the IR-stretching frequencies follow the same ordering of the sigma-donating character of the borane. The electron density on the borane hydrogen should increase with increasing sigma donation from the substituents. This increase in hydridic character should shorten the M−H distance, which apparently leads to the pivoting of the borane about the B−H bond. Steric effects may also contribute to the lengthening of the M−B distance. However, space-filling models of the structures of the complexes suggest that steric effects between the borane substituents and the small $MeCpMn(CO)_2$ fragment are not strong.

5. Dynamic Processes. Rapid site exchange processes were revealed by ^{13}C NMR spectroscopy. The room temperature ^{13}C NMR spectrum of **1** showed only one carbonyl resonance (226.4 ppm) and two methine carbons in the catechol backbone. These data showed that the intramolecular motion A shown in Figure 11, and perhaps motion B, were occurring in **1** at room temperature. Cooling of **1** in THF-d_8 to −115 °C led to decoalescence of the carbonyl resonance into two signals of equal intensity (225.1 and 230.5 ppm, T_c = 173 K). The catechol backbone, however, showed two methine resonances at this temperature, as it did at room temperature. Assuming the catecholate resonances could be resolved in a frozen structure, motion B appears to occur on the NMR time scale, even at −115 °C. The two methine carbon atoms in the MeCp ligand, which are diastereotopic, were not distinct in solution at even

(33) Nöth, H.; Wrackmeyer, B. *Nuclear Magnetic Resonance Spectroscopy of Boron Compounds*; Springer: Berlin, 1978; p 461.

(34) Mann, B. E.; Taylor, B. F. *Organometallic Chemistry: ^{13}C NMR Data for Organometallic Compounds*; Academic Press: London, 1981; pp 225−227.

−115 °C, most likely because of their small differences in chemical shift.[34] From the data for the carbonyl signals, an activation barrier of $\Delta G^{\ddagger} = 7.4 \pm 1.2$ kcal/mol can be estimated for motion A in Figure 11. This value is in good agreement with the rotational barriers of other σ-donor/π-acceptor ligands on $CpM(CO)_2$ fragments such as substituted and unsubstituted olefins and acetylenes; in these cases the rotational barriers are 8−10 kcal/mol.[35−37]

Ligand-Substitution Reactions and Mechanistic Studies. Several ligand-substitution reactions were performed to probe potential reversibility of borane coordination and to assess the relative stabilities of σ-borane, silane, and stannane complexes of the $(MeCp)Mn(CO)_2$ 16-electron fragment. Borane complex **1** reacted with excess $HSiPh_2Me$ or $HSnPh_3$ to form the corresponding silyl hydride[21] and stannane[38,39] complexes in good yields. The stannane derivative is thermally much more stable than the borane complex, which is similar in stability to the silyl hydride. Although evaluated only qualitatively, the equilibria between borane and silane or stannane complexes favored the silyl hydride and stannane complexes and free borane.

Detailed kinetic studies were undertaken of the reaction of catecholborane complex **1** with diphenylacetylene. The reaction showed a first-order dependence on the concentration of complex **1** (Figure 5), and the observed reaction rates depended on the concentrations of both the catecholborane and the diphenylacetylene. Added catecholborane was found to retard the reaction. Reactions conducted with increasing concentrations of PhCCPh revealed saturation behavior (Figure 6). The reaction was first-order in [PhCCPh] at low [PhCCPh], but became zero-order in this reagent when its concentration was much higher than the added borane concentration. Similar kinetic behavior was observed for the reaction of the silane complex $CpMn(CO)_2(HSiPh_3)$ with PPh_3.[40] This rate behavior is characteristic of dissociative ligand-substitution reactions. It is consistent with the mechanism in Scheme 4, which is described by the rate expression in eq 1. At high concentrations of PhCCPh, this expression reduces to a first-order expression where $k_{obs} = k_1$. The observed rate constant can also be expressed as in eq 2.

$$\frac{d[(MeCp)Mn(CO)_2(HBcat)]}{dt} = \frac{k_1 k_2[PhCCPh]}{k_2[PhCCPh] + k_{-1}[HBcat]}[(MeCp)Mn(CO)_2(HBcat)] = -k_{obs}[(MeCp)Mn(CO)_2(HBcat)]$$

$$\text{with } k_{obs} = \frac{k_1 k_2[PhCCPh]}{k_2[PhCCPh] + k_{-1}[HBcat]} \quad (1)$$

$$\frac{1}{k_{obs}} = \frac{1}{k_1} + \frac{k_{-1}\ [HBcat]}{k_1 k_2[PhCCPh]} \quad (2)$$

Values for k_1, the rate constant for dissociation of the borane ligand, and for k_2/k_{-1}, the partitioning of the 16-electron intermediate for formation of an alkyne complex and a borane complex, are provided in Figure 7 and are derived from the plot of $1/k_{obs}$ versus [HBcat] at a constant [PhCCPh]. The selectivity for the reaction of the unsaturated fragment with PhCCPh versus borane ($k_2/k_{-1} = 6.8$) was low, considering the greater stability of the alkyne complex. Presumably, the high reactivity of the 16-electron intermediate makes it relatively unselective. The electrophilic nature of the borane may also accelerate its reaction with the electron-rich Mn(I) intermediate.[40]

Scheme 4

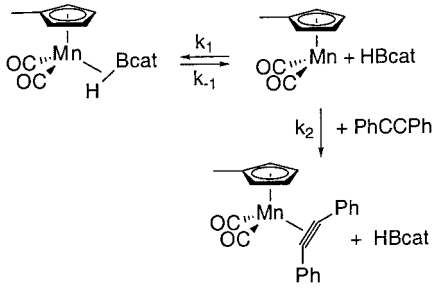

In addition to reaction orders, Eyring activation parameters were obtained for the ligand-displacement reaction. We obtained the activation parameters with a high concentration of PhCCPh so that the value of $k_{obs} = k_1$. The enthalpy of activation for k_1, $\Delta H^{\ddagger} = 24$ kcal/mol, provides an upper limit for the Mn−(HBcat) bond-dissociation energy. The $\Delta H^{\ddagger}$ value is slightly lower than that for the dissociation of triphenylsilane from $(MeCp)Mn(CO)_2(HSiPh_3)$ (25.5 kcal/mol) and significantly higher than the enthalpy of binding in most η^2-H_2 complexes (13−17 kcal/mol).[41] A very similar dissociation enthalpy of 25 ± 3 kcal/mol was found for the dissociation of catecholborane from the titanocene fragment.[12] Eyring activation parameters were also obtained for the reaction of dicyclohexylborane complex **4,** and $\Delta H^{\ddagger}$ for the k_1 step was 21 kcal/mol, indicating a metal−borane binding energy that is roughly 4 kcal/mol weaker than that in the catecholborane complex. As mentioned above, space-filling models do not indicate strong differences in steric properties of **1**, **2**, and **4**. This information suggests that electronic differences account for the relative stabilities of **1** and **4**. Although complex **3** may decompose by pathways other than simple borane dissociation, its pronounced thermal instability is consistent with this assertion.

Conclusion

The synthesis and isolation of σ-borane complexes of manganese and rhenium show that σ-borane complexes are not restricted to early transition metals such as titanium and can encompass many or all of the transition metals. These complexes can be constructed in three different ways: coordination of a metal fragment to the free borane, alcoholysis of a bis-boryl complex, or borylation of an anionic metal-hydride complex. The thermal stability of the borane complexes of manganese is comparable to that of other σ-complexes of Mn(I) and is significantly higher than that for titanocene−borane complexes. The most important difference between σ-borane compounds and X−H σ-complexes of ligands with saturated elements X is the availability of a free p-orbital at boron. This orbital allows for back-donation from the HOMO of the metal fragment into the boron.[12] In alkane, silane, or stannane complexes, back-donation occurs into the H−X σ*-orbital, which is much higher in energy than the borane p-orbital.

(35) Alt, H.; Herberhold, M.; Kreiter, C. G.; Strack, H. *J. Organomet. Chem.* **1974**, *77*, 353.
(36) Herberhold, M.; Kreiter, C. G.; Stüber, S.; Wiedersatz, G. O. *J. Organomet. Chem.* **1975**, *96*, 89.
(37) Faller, J. W.; Johnson, B. V. *J. Organomet. Chem.* **1975**, *88*, 101.
(38) Khaleel, A.; Klabunde, K. J.; Johnson, A. *J. Organomet. Chem.* **1999**, *572*, 11.
(39) Lee, S. W.; Yang, K.; Martin, J. A.; Bott, S. G.; Richmond, M. G. *Inorg. Chim. Acta* **1995**, *232*, 57.
(40) Hart-Davis, A. J.; Graham, W. A. G. *J. Am. Chem. Soc.* **1971**, *93*, 4388.
(41) Heinekey, D. M.; Oldham, W. J. *Chem. Rev.* **1993**, *93*, 913.

Experimental Section

General considerations. Unless otherwise noted, all manipulations were conducted using standard Schlenk techniques or in an inert atmosphere glovebox. ^{1}H NMR spectra were obtained on either a GE QE 300 MHz or a GE Ω 300 MHz Fourier transform spectrometer. ^{13}C NMR spectra were recorded on either a Bruker AM 500 MHz or a GE QE 300 MHz spectrometer. ^{11}B and ^{2}H NMR spectra were obtained on the GE Ω 300 spectrometer operating at 96.38 and 46.13 MHz, respectively. ^{1}H NMR spectra were recorded relative to residual protiated solvent. ^{11}B NMR spectra were recorded in units of parts per million relative to BF_3·Et_2O as an external standard.

Unless specified otherwise, all reagents were purchased from commercial suppliers and used without further purification. K[(MeCp)Mn(CO)$_2$H],[21] *B*-chloro-pinacolborane,[42] *B*-deuterio-catecholborane,[43] and *cis*-Cp*Re(CO)$_2$(Bpin)$_2$[26] were prepared using literature procedures. *B*-Chloro-pinacolborane was used in situ as prepared and was not isolated. Protiated solvents were distilled from purple solutions containing sodium and benzophenone. Deuterated solvents were dried similarly but were collected by vacuum transfer. Reaction yields that were obtained by ^{1}H NMR spectroscopy were determined by using C_6Me_6 as the internal standard.

Photochemical reactions were conducted using a Hanovia 450 W medium-pressure mercury-arc lamp placed in a Pyrex immersion well.

Preparation of (MeCp)Mn(CO)$_2$(HBcat) (1). (a) Photochemical Synthesis. (MeCp)Mn(CO)$_3$ (500 mg, 2.3 mmol) was dissolved in 80 mL of THF, and 3.30 g (27.5 mmol) of catecholborane were added. The solution was irradiated for 30 min at room temperature. The solvent was evaporated from the deep-yellow solution, and a dark-yellow oil was obtained. Pentane (50 mL) was added, the solution was filtered, and its volume was reduced to 4 mL. This concentrated solution was stored at −30 °C for 14 h, and the resulting yellow solid was recrystallized from pentane to obtain yellow crystals of **1** in 53% yield (0.378 g).

(b) Salt extrusion. K[(MeCp)Mn(CO)$_2$H] (1.00 g, 4.3 mmol) was suspended in 30 mL of pentane, and 0.67 g (4.3 mmol) of *B*-chlorocatecholborane were added with vigorous stirring. Immediate formation of KCl was observed, and the solution turned yellow. After 10 min, the reaction mixture was filtered, reduced in volume, and stored at −30 °C for 14 h. The product was recrystallized from pentane to provide 1.286 g of **1** as a microcrystalline powder (92% yield). ^{1}H NMR (C_6D_6): δ 7.04 (m, 2H), 6.77 (m, 2H), 4.15 (s, 2H), 4.07 (s, 2H), 1.50 (s, 3H), −14.46 (br, 1H). ^{13}C NMR (THF-d_8): δ 226.1, 151.2, 121.4, 110.5, 104.1, 83.8, 83.4, 12.7. ^{11}B NMR (C_6D_6): δ 46 (s, br). A value $^1J(^1H,^{11}B)$ of 98 Hz was obtained from a high temperature ^{11}B NMR spectrum (T = 373 K). IR (hexanes, cm^{-1}): 1995 (ν_sCO, s), 1937 (ν_{as}CO, s), 1606 (m, br). Anal. Calcd for $C_{14}H_{12}BMnO_4$: C, 54.25; H, 3.91. Found: C, 54.02; H, 3.86.

Preparation of (MeCp)Mn(CO)$_2$(DBcat) (1-*d*). The deuterio analogue of **1** was prepared in 48% yield in a manner similar to the photochemical preparation of **1** but using DBcat. ^{2}H NMR (C_6H_6): δ −14.4 (s, br, 1D). ^{11}B NMR (C_6H_6): δ 46 (s, br). IR (hexanes, cm^{-1}): 1146 (m, br).

Preparation of (MeCp)Mn(CO)$_2$(HBpin) (2). (a) Photochemical Synthesis. Pinacolborane complex **2** was synthesized as described for the photochemical preparation of **1**, starting with 0.500 g (2.3 mmol) of (MeCp)Mn(CO)$_3$. Yield: 0.132 g (18%).

(b) Salt Extrusion. A solution of *B*-chloropinacolborane in pentane was generated by the addition of 1.0 mL (1.0 mmol) of a 1.0 M solution of BCl_3 in heptane to a stirred solution of 0.118 g (1.0 mmol) of pinacol in 5 mL of pentane. A white precipitate that formed during the addition was removed by filtration, and the filtrate was used as obtained. This filtrate was added to a suspension of 0.175 g (0.8 mmol) of K[(MeCp)Mn(CO)$_2$H] in 8 mL of pentane. After 30 min, the solution was filtered, and the solvent was evaporated under reduced pressure. The resulting yellow solid was recrystallized twice from pentane, and yellow crystals were obtained. Yield: 0.157 g (65%). ^{1}H NMR (C_6D_6): δ 4.22 (s, 2H), 4.13 (s, 2H), 1.61 (s, 3H), 1.14 (s, 12H), −15.66 (br, 1H). ^{13}C NMR (THF-d_8): δ 221.1, 104.9, 83.8, 82.8, 79.9, 29.9, 13.7. ^{11}B NMR (C_6D_6): δ 45 [d, $^1J(^1H,^{11}B)$ = 88 Hz]. IR (hexanes, cm^{-1}): 1983 (ν_sCO, s), 1921 (ν_{as}CO, s), 1603 (m).

Preparation of (MeCp)Mn(CO)$_2$(HBMe$_2$) (3). K[(MeCp)Mn(CO)$_2$H] (0.050 g, 0.2 mmol) was suspended in 1.5 mL of pentane, and 0.021 mL (0.2 mmol) of $BrBMe_2$ were added with vigorous stirring. After 10 min, the red mixture was filtered, and the solvent was evaporated under reduced pressure. Compound **4** was obtained as a red oil, which was judged to be pure by NMR spectroscopy. Yield: 0.042 g (82%). ^{1}H NMR (C_6D_6): δ 4.10 (s, 2H), 3.99 (s, 2H), 1.42 (s, 3H), 1.21 (s, 6H), −17.06 (br, 1H). ^{13}C NMR (C_6D_6): δ 226.9, 103.5, 85.0, 84.4, 24.3(br), 13.2. ^{11}B NMR (C_6D_6): δ 101 (s). IR (hexanes, cm^{-1}): 1975 (ν_sCO, s), 1910 (ν_{as}CO, s), 1592 (m).

Preparation of (MeCp)Mn(CO)$_2$(HBCy$_2$) (4). K[(MeCp)Mn(CO)$_2$H] (0.050 g, 0.2 mmol) was suspended in 1.5 mL of pentane, and 0.220 mL (0.2 mmol) of a 1.0 M solution of $ClBCy_2$ in hexanes were added with vigorous stirring. The mixture turned red immediately. After 10 min, the reaction was filtered, and the solvent was evaporated under reduced pressure. The borane complex was obtained as a red microcrystalline solid. Yield: 0.069 g (85%). ^{1}H NMR (C_6D_6): δ 4.28 (s, 2H), 4.08 (s, 2H), 1.1−1.9 (m, 25H), −16.96 (br, 1H). ^{13}C NMR (C_6D_6): δ 226.6, 102.7, 85.3, 84.3, 48.3(br), 30.4, 28.2, 27.3, 13.3. ^{11}B NMR (C_6D_6): δ 104 (s). IR (hexanes, cm^{-1}): 1967 (ν_sCO, s), 1901 (ν_{as}CO, s), 1597 (m).

Preparation of Cp*Re(CO)$_2$(HBpin) (5). *cis*-Cp*Re(CO)$_2$(Bpin)$_2$ (0.046 g, 0.07 mmol) was dissolved in 1.0 mL of benzene, and 2.9 μL (0.07 mmol) of methanol were added slowly. After stirring for 2 h the volatile materials were removed, and a colorless solid remained. This solid was recrystallized from 0.5 mL of pentane at −30 °C. Cp*Re(CO)$_2$(HBpin) was obtained in quantitative yield (0.037 g). The reaction also proceeds with other alcohols but the use of methanol allowed for evaporation of the MeOBpin byproduct under reduced pressure. ^{1}H NMR (C_6D_6): δ 1.88 (s, 15H), 1.15 (s, 12H), −11.06 (br, 1H). ^{11}B NMR (C_6D_6): δ 46 (s). IR (hexanes, cm^{-1}): 1981 (ν_sCO, s), 1924 (ν_{as}CO, s), 1603 (m).

Ligand-Substitution Reactions. (a) Thermal Reactions. (MeCp)Mn(CO)$_2$(HBcat) (15 mg, 0.048 mmol) and 3.9 mg (0.024 mmol) of C_6Me_6 as an internal standard were dissolved in 0.6 mL of C_6D_6. Five equiv of the appropriate incoming ligand were added. In the case of the reaction with CO, 2 atm of CO were added. The mixtures were reacted at 60 °C for 2 h in an NMR sample tube. Yields of product were determined by comparison of the reactant and product ^{1}H NMR integrals versus those for the internal standard.

(b) Photochemical Reactions. Samples were prepared as described for the thermal reactions. For the reaction with $HSiPh_2Me$, C_6D_6 was used as a solvent; for reaction with pinacolborane, THF-d_8 was used. The solutions were irradiated in NMR sample tubes for 30 min at room temperature. The following compounds were obtained in the yields provided in parentheses: (MeCp)Mn(CO)$_2$(HBpin) (**2**) (69%), (MeCp)Mn(CO)$_2$($HSiPh_2Me$) (94%), (MeCp)Mn(CO)$_2$(PhCCPh) (94%), (MeCp)Mn(CO)$_2$($HSnPh_3$) (91%) and (MeCp)Mn(CO)$_3$ (92%).

Kinetic Studies of the Reaction of 1 with PhCCPh. All experiments were monitored at 70 °C by UV/vis spectroscopy at a wavelength of λ = 420 nm, which is the absorption maximum of the diphenylacetylene complex formed in the reaction. Data were fit to a single exponential for the disappearance of starting material.

(a) Dependence of the Reaction Rate on the Concentration of Catecholborane. A stock solution was prepared containing 4.0 mg (0.013 mmol) of **1** and 34.6 mg (0.194 mmol) of PhCCPh in 20.0 mL of toluene. For each individual experiment, 3.0 mL of the stock solution were used, and 1.02 μL (0.009 mmol), 4.08 μL (0.038 mmol), 8.16 μL (0.077 mmol), 16.32 μL (0.153 mmol), or 24.48 μL (0.230 mmol) of catecholborane were added to the aliquots.

(b) Dependence of the Reaction Rate on the Concentration of PhCCPh. A stock solution was prepared containing 3.0 mg (0.009 mmol) of **1** and 20.0 μL (0.167 mmol) of catecholborane in 40.0 mL of toluene. For each individual experiment, 3.0 mL of the stock solution were used, and 1.0 mg (0.006 mmol), 2.0 mg (0.011 mmol), 4.0 mg (0.022 mmol), 8.0 mg (0.045 mmol), 32.0 mg (0.180 mmol), or 64.0 mg (0.360 mmol) of PhCCPh were added to the aliquots.

(c) Measurement of Eyring Parameters. A stock solution was prepared containing 3.0 mg (0.009 mmol) of **1**, 20 μL (0.167 mmol)

(42) Herberich, G. E.; Fischer, A. *Organometallics* **1996**, *15*, 58.
(43) Männig, D.; Nöth, H. *J. Chem. Soc., Dalton Trans.* **1985**, 1689.

of catecholborane and 105 mg (0.590 mmol) of PhCCPh in 20.0 mL of toluene. Individual experiments were run at 55, 60, 65, 75, and 85 °C with 3.0 mL of the stock solution

Kinetic Studies of the Reaction of 4 with PhCCPh. All experiments were monitored by UV/vis spectroscopy at a wavelength of $\lambda =$ 440 nm. Data were fit to a single exponential for the disappearance of starting material. Eyring measurement: A stock solution was prepared containing 5.0 mg (0.014 mmol) of **1** and 181 mg (1.017 mmol) of PhCCPh in 20.0 mL of toluene. Individual experiments were run at 25, 35, 40, 45, 50, and 55 °C with 3.0 mL of the stock solution.

Preparation of Dicyclohexyl-*cis*-1,2-diphenyl(vinyl)borane. To a solution of 50.0 mg (0.28 mmol) of diphenylacetylene in 1.0 mL of toluene, 50.0 mg (0.28 mmol) of dicyclohexylborane[44] were added, and the solution was stirred at room temperature for 15 min. The solvent was evaporated under reduced pressure, and the remaining solid was recrystallized from diethyl ether at −35 °C. The dicyclohexyl-*cis*-1,2-diphenyl(vinyl)borane was obtained as a colorless, microcrystalline solid in 92% yield (92 mg). ^{1}H NMR (C_6D_6): δ 1.2−1.5 (m, 11 H), 1.6−1.8 (m, 11H), 6.78 (s, 2H), 6.95−7.10 (m, 4H), 7.15−7.25 (m, 4H), 7.41 (s, 1H). ^{11}B NMR (C_7D_8): δ 76 (s).

Crystallographic Analysis of 1. Yellow single crystals of **1** that were suitable for X-ray diffraction studies were obtained by cooling a solution of **1** in pentane at −30 °C for 2 days. X-ray diffraction data for **1** were obtained at 183 K with graphite monochromatic Mo Kα radiation. Crystal data are provided in Table 1. A total of 4797 reflections were collected, 3465 of which were unique ($R_{int} = 0.030$). The space group was determined to be $P\bar{1}$. For $Z = 2$ and FW = 309.99, the calculated density was 1.57 g/cm^3. A SORTAV absorption correction was applied. The structure was solved by heavy-atom Patterson methods and was expanded using Fourier techniques. H1 was located on the difference Fourier map. The non-hydrogen atoms were refined anisotropically. Hydrogen atoms were refined isotropically. The final cycle of full-matrix least-squares refinement was based on 3091 observed reflections ($I > 3.00\sigma(I)$) and 229 variable parameters and converged with unweighted and weighted agreement factors of $R =$ 3.0% and $R_w = 4.4\%$. The crystallographic data of **1** were deposited in the Cambridge Crystallographic Data Center under reference code 147133.

Crystallographic Analysis of 2. Yellow single crystals of **2** that were suitable for X-ray diffraction studies were obtained by cooling a solution of **2** in pentane at −30 °C for 4 days. X-ray diffraction data for **2** were taken at 183 K with graphite monochromatic Mo Kα radiation. Crystal data are provided in Table 1. A total of 4421 reflections was collected. The space group was determined to be $P2_1/a$. For $Z = 4$ and FW = 318.06, the calculated density was 1.43 g/cm^3. The structure was solved by heavy-atom Patterson methods and expanded using Fourier techniques. H1 was located on the difference Fourier map. The non-hydrogen atoms were refined anisotropically. Some hydrogen atoms, including H1, were refined isotropically, while the rest were included in fixed positions. The final cycle of full-matrix least-squares refinement was based on 3551 observed reflections [$I > 5.00\sigma(I)$] and 185 variable parameters and converged with unweighted and weighted agreement factors of $R = 3.1\%$ and $R_w = 4.9\%$. The crystallographic data of **2** were deposited Cambridge Crystallographic Data Center under reference code 147134.

Crystallographic Analysis of 4. Red single crystals of **4** that were suitable for X-ray diffraction studies were obtained by cooling a solution of **4** in pentane:toluene 9:1 at −30 °C for 3 days. X-ray diffraction data for **4** were taken at 183 K with graphite monochromatic Mo Kα radiation. Crystal data are provided in Table 1. A total of 4323 reflections was collected. The space group was determined to be $P\bar{1}$. For $Z = 2$ and FW = 368.20, the calculated density was 1.27 g/cm^3. The structure was solved by direct methods and expanded using Fourier techniques. H1 was located on the difference Fourier map. The non-hydrogen atoms were refined anisotropically. Some hydrogen atoms, including H1, were refined isotropically, and the rest were included in fixed positions. In the case of the methyl-group hydrogen atoms, one hydrogen was located in the difference map and included at an idealized distance to set the orientation of the other two hydrogen atoms. The final cycle of full-matrix least-squares refinement was based on 3097 observed reflections [$I > 5.00\sigma(I)$] and 221 variable parameters and converged with unweighted and weighted agreement factors of $R =$ 3.7% and $R_w = 5.0\%$. The crystallographic data of **4** were deposited in the Cambridge Crystallographic Data Center under reference code 147135.

Acknowledgment. We thank Susan DeGala for the crystal structure analyses of compounds **1**, **2**, and **4**. The NSF is gratefully acknowledged for supporting this work. S.S. thanks the Deutsche Forschungsgemeinschaft for a postdoctoral fellowship.

Supporting Information Available: Data for compounds **1**, **2**, and **4**. This material is available free of charge via the Internet at http://pubs.acs.org.

JA001546O

(44) Pelter, A.; Smith, K.; Brown, H. C. *Borane Reagents*; Academic Press: London, 1988; p 426.